ResearchGate

See discussions, stats, and author profiles for this publication at: https://www.researchgate.net/publication/7645749

Formation of Polyelectrolyte Multilayer Architectures with Embedded DMPC Studied in Situ by Neutron Reflectometry

ARTICLE *in* LANGMUIR · SEPTEMBER 2005

Impact Factor: 4.46 · DOI: 10.1021/la050407n · Source: PubMed

CITATIONS
48

READS
34

5 AUTHORS, INCLUDING:

Thomas Gutberlet
Forschungszentrum Jülich
143 PUBLICATIONS **1,735** CITATIONS
SEE PROFILE

Helmuth Moehwald
Max Planck Institute of Colloids and Interfaces
1,004 PUBLICATIONS **38,672** CITATIONS
SEE PROFILE

Available from: Thomas Gutberlet
Retrieved on: 31 January 2016

Formation of Polyelectrolyte Multilayer Architectures with Embedded DMPC Studied in Situ by Neutron Reflectometry

Christophe Delajon,[†,‡] Thomas Gutberlet,[§] Roland Steitz,[⊥] Helmuth Möhwald,[†] and Rumen Krastev*[,†,||]

Max-Planck Institute of Colloids and Interfaces, Wissenschaftspark Golm, 14424 Potsdam, Germany, ISIS-Université Louis Pasteur, 8 Allée G. Monge, BP 70028, 67083 Strasbourg, France, Paul Scherrer Institute, 5232 Villigen PSI, Switzerland, and Hahn-Meitner Institute, Berlin, Glienicker Strasse 100, 14109 Berlin, Germany

Received February 15, 2005. In Final Form: June 24, 2005

The coupling of lipid molecules to polymer components in a planar biomimetic model membrane made of a lipid bilayer (dimyristoylphosphatidylcholine) supported by polyelectrolyte multilayers is studied. The polyelectrolyte support was prepared by layer-by-layer deposition of positively charged poly(allylamine hydrochloride) (PAH) and negatively charged poly(sodium 4-styrenesulfonate) (PSS). Two polymer sample terminations were considered: positively charged (PAH-terminated) and negatively charged (PSS-terminated). Neutron reflectometry studies showed that, whereas positively charged samples did not favor the deposition of lipid, negatively charged samples allowed the deposition of a lipid bilayer with a thickness of ∼5 nm. In the latter case, formation of polyelectrolyte layers after the deposition of the lipid layer was also possible.

Introduction

Biomimetic surfaces with tailored properties are a major object of application-oriented biophysical studies. Thin membranes of defined composition, thickness, and structure find broad applications ranging from coating of surfaces to filtration and encapsulation. Hybrid systems between biological and artificial materials are sought, since they allow one to combine the unmatched functionality of natural macromolecules with a potential for tailoring the thickness and the shape of coatings.[1] Different studies showed that the deposition of free lipid layers was possible as monolayers on top of polymers[2,3] as bilayers on top of natural polymers with Langmuir−Blodgett techniques[4] or with a lipid vesicle deposition process on top of colloidal particles.[5] Most of the studies concerning lipid−polymer systems deal with functional lipids polymerized or bound to a polymeric backbone,[6−9] and only a few deal with "free" lipid bilayers in contact with polymers.[10−12]

Polyelectrolyte (PE) multilayers (PEM) adsorbed on solid support were introduced as highly versatile surface coatings.[13] The multilayer formation is based on the layer-by-layer (LbL) deposition technique,[14] which exploits the fact that polyelectrolytes adsorb onto surfaces of opposite charge and that the surface charge density is reversed by this process. Therefore, a multilayer can be built up by alternating adsorption of positively and negatively charged polyelectrolytes. The thickness of such multilayers can be controlled down to molecular dimensions and varied by the number of adsorption cycles, salt concentration of the PE solutions, and with fine-tuning carried out by the modification of the adsorption conditions.[15] Interestingly, the coatings can also be used to form free-standing membranes[16] or even hollow microcapsules.[17] In this latter case, it can be accomplished by the use of appropriate substrates for the coating, which allow a subsequent dissolution under conditions that do not destroy the multilayer. This permits their application for filtration or encapsulation.

Neutron reflectometry (NR) is a powerful technique for studying adsorption at surfaces. It provides detailed information about the structure and composition of the

* Corresponding author. Phone: ++49(0)331 567 9232. E-mail: krustev@mpikg.mpg.de.
† Max-Planck Institute of Colloids and Interfaces.
‡ ISIS-Université Louis Pasteur.
§ Paul Scherrer Institute.
⊥ Hahn-Meitner Institute.
|| Former address: Hahn Meitner Institute, Berlin, Glienicker Str. 100, 14109 Berlin, Germany.

(1) Sackmann, E. *Science* **1995**, *271*, 43−48.
(2) de Meijere, K.; Brezesinski, G.; Pfohl, T.; Möhwald, H. *J. Phys. Chem. B* **1999**, *103*, 8888−8893.
(3) Elliott, J. T.; Burden, D. L.; Woodward, J. T.; Sehgal, A.; Douglas, J. F. *Langmuir* **2003**, *19*, 2275−2283.
(4) Baumgart, T.; Offenhausser, A. *Langmuir* **2002**, *19*, 1730−1737.
(5) Moya, S.; Donath, E.; Sukhorukov, G. B.; Auch, M.; Baumler, H.; Lichtenfeld, H.; Möhwald, H. *Macromolecules* **2000**, *33*, 4538−4544.
(6) McArthur, S. L.; Halter, M. W.; Vogel, V.; Castner, D. G. *Langmuir* **2003**, *19*, 8316−8324.
(7) Liu, H.; Faucher, K. M.; Sun, X. L.; Feng, J.; Johnson, T. L.; Orban, J. M.; Apkarian, R. P.; Dluhy, R. A.; Chaikof, E. L. *Langmuir* **2002**, *18*, 1332−1339.
(8) Perez-Salas, U. A.; Faucher, K. M.; Majkrzak, C. F.; Berk, N. F.; Krueger, S.; Chaikof, E. L. *Langmuir* **2003**, *19*, 7688−7694.
(9) Xie, A. F.; Granick, S. *Nat. Mater.* **2002**, *1*, 129−133.
(10) Wong, J. Y.; Majewski, J.; Seitz, M.; Park, C. K.; Israelachvili, J. N.; Smith, G. S. *Biophys. J.* **1999**, *77*, 1445−1457.
(11) Kügler, R.; Knoll, W. *Bioelectrochemistry* **2002**, *56*, 175−178.
(12) Gutberlet, T.; Klösgen, B.; Krastev, R.; Steitz, R. *Adv. Eng. Mater.* **2004**, *6*, 832−836.
(13) Decher, G.; Schlenoff, J. B. *Multilayer Thin Films: Sequential Assembly of Nanocomposite Materials*; Wiley-VCH Verlag GmbH: Weinheim, 2003.
(14) Decher, G. *Science* **1997**, *277*, 1232−1237.
(15) Lösche, M.; Schmitt, J.; Decher, G.; Bouwman, W. G.; Kjaer, K. *Macromolecules* **1998**, *31*, 8893−8906.
(16) Sukhorukov, G. B.; Schmitt, J.; Decher, G. *Ber. Bunsen-Ges.* **1996**, *100*, 948−953.
(17) Sukhorukov, G. B.; Donath, E.; Lichtenfeld, H.; Knippel, E.; Knippel, M.; Budde, A.; Möhwald, H. *Colloids Surf. A* **1998**, *137*, 253−266.

10.1021/la050407n CCC: $30.25 © 2005 American Chemical Society
Published on Web 07/28/2005

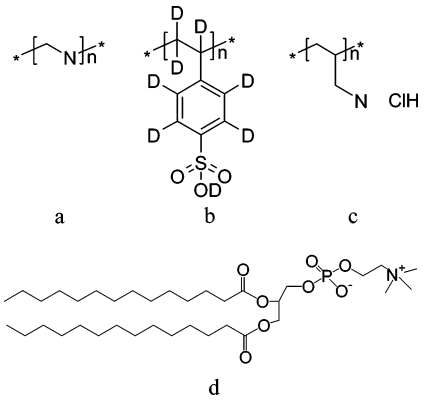

Figure 1. Chemicals used: (a) PEI, (b) d-PSS, (c) PAH, and (d) DMPC.

adsorbed layers.[18,19] NR allows measuring the composition profiles along the z direction normal to the interface over a length scale up to 500 nm, with a resolution down to ~0.2 nm. Because neutrons only weakly interact with most materials, in situ measurements at solid/liquid interfaces can be performed. An important advantage of the NR method is the absence of sample damage, even upon prolonged exposure to the neutron beam. The specular neutron reflectivity method is based on the variation of the specular reflection, R, at the interface between two phases with the variation of the wave vector transfer, $Q = (4\pi/\lambda) \sin \theta$, where θ is the angle of incidence of the neutron beam and λ is the neutron wavelength. The variation depends on the interfacial composition perpendicular to the layer interface characterized by the neutron scattering length density (SLD) $\rho(z) = \sum n_i b_i$. Here n_i is the number density of the element i, and b_i is its scattering length. Different isotopes are characterized by different values of the coefficient b_i. The use of compounds with different isotopes of a same chemical element allows NR measurements to be focused on particular parts of a thin layer without perturbing the whole chemical structure.

NR experiments were performed in the present work to follow the process of formation and the organization of dimyristoylphosphatidylcholine (DMPC) zwitterionic lipid layers on top of PEM films. First, we present the results of the adsorption of the DMPC onto a positively or negatively terminated PEM block prepared from perdeuterated poly(sodium 4-styrenesulfonate) (d-PSS) and poly(allylamine hydrochloride) (PAH). The data are analyzed in terms of thickness and SLD. Further, we demonstrate the possibility to continue the deposition of PE layers after the lipid deposition.

Experimental Section

Chemicals. (cf. Figure 1) Poly(ethylenimine) (PEI) (M_w 7.5 × 10^4 g mol^{-1}) and poly(allylamine hydrochloride) (PAH) (M_w 7 × 10^4 g mol^{-1}) were purchased from Sigma-Aldrich. Perdeuterated poly(sodium 4-styrenesulfonate) (d-PSS) (M_w 8.03 × 10^4 g mol^{-1}) was purchased from Polymer Standards Service (Mainz, Germany). Dimyristoylphosphatidylcholine (DMPC) (M_w 6.77 × 10^2 g mol^{-1}) was purchased from Sigma-Aldrich. Sodium chloride (pro analysis grade) was purchased from Riedel-de Haën. Deuterium oxide (min. 99.9% isotope enrichment) was purchased from Sigma-Aldrich.

All chemicals were used without further purification. The aqueous solutions were prepared with ultrapure water from a Milli-Q Plus 185 water generation system (Millipore, resistivity >18.2 MΩ cm).

Substrates. Silicon blocks from Siliciumbearbeitung Andrea Holm (Tann/Ndb., Germany) with two sides polished (dimensions 8 × 5 × 1.5 cm^3, orientation ⟨100⟩), were used for the NR experiments. They were cleaned by treatment in a hot piranha solution (35 wt % H_2O_2/85 vol % H_2SO_4 (1:1) v/v, ~80 °C) for 20 min (*Caution: piranha solution is extremely corrosive.*) and then thoroughly washed with ultrapure water.

PE Multilayer Buildup (Adsorption of PE on flat silicon substrates). The substrates were coated with PE using the LbL technique described in ref 14. PEI was dissolved in ultrapure water and was used as a precursor to enhance the stability of the alternating adsorbed d-PSS/PAH multilayers. d-PSS and PAH were dissolved in 1 M NaCl solutions. The concentration of the PE solutions was 10^{-2} monomol L^{-1}. The clean hydrophilic Si substrates were dipped alternatively in a beaker containing the polycation or the polyanion solution for 20 min. The substrates were rinsed in ultrapure water for 2 min in three different beakers to remove excess polymer after each adsorption step. The cycle was repeated until the desired number of layers had been achieved. Two PEM structures were prepared: structure dP$^+$, PEI/(d-PSS/PAH)$_6$ (13 PE layers, PAH-terminated) and structure dP$^-$, PEI/(d-PSS/PAH)$_6$/d-PSS (14 PE layers, PSS-terminated).

Lipid Small Unilamellar Vesicles (SUV) Suspension. The lipid SUV suspension was obtained by first dissolving 100 mg of DMPC in a 1:1 v/v mixture of chloroform and methanol in a glass vessel. The organic solvent was then gently removed by using a rotative evaporator. The lipid film obtained on the walls of the vessel was dried under vacuum for more than 48 h. Ultrapure water was then added to hydrate the film by 100-μL aliquots up to a total volume of 2 mL, followed each time by a 3-min immersion in an ultrasonic bath (temperature 313 K (40 °C)). This intermediate solution was extruded 21 times through a 200-nm pore diameter polycarbonate filter and then 21 times through a 100-nm pore diameter polycarbonate filter (Avestin Inc., Ottawa, Canada) to obtain SUV and then diluted to 0.5 g × L^{-1} to obtain the final lipid suspension.

In Situ Deposition. The solid/liquid experimental cell (see the Supporting Information) used in the NR experiments allowed the liquid (typical volume ~10 mL) in contact with the solid interface to be exchanged. The cell was linked to an external water bath to maintain the temperature at 299 ± 1 K (26 °C). The SUV suspension was used for formation of a lipid layer on top of the previously prepared PE multilayers. An excess volume of the suspension was injected slowly (15 mL in ~60 s) into the cell. This was followed by a delay ("incubation time") of 30 min and then rinsing with an excess of D_2O. The same procedure was used for the formation of PE layers on top of the lipid layer, except that the incubation time was 20 min.

Neutron Reflectometry. The reflectivity, R, which is the ratio between the intensity of the incoming and the reflected beam, was measured as a function of Q. The experiments were performed with D_2O on the bottom of the experimental cell against a Si block above. In this case the lower medium has a higher SLD than the upper one. Under these conditions, $R = 1$ for Q below a critical value Q_c. Above Q_c, R decays with Q, and the shape of the dependence is a function of the area-averaged scattering length density profile normal to the interface. A beam of rectangular cross section was set by a slit system on the sample side. Two different reflectometers were used. At the V6 monochromatic (wavelength $\lambda = 0.47$ nm) reflectometer[20,21] at the Hahn-Meitner Institute, Berlin, Germany, the studies were performed in a $\theta/2\theta$ geometry. At the neutron reflectometer AMOR at the Paul Scherrer Institute, Villigen, Switzerland,[22−24] the experiments were performed in time-of-flight (ToF) mode at three angles of incidence (0.4, 0.9, and 1.5°), covering the whole necessary Q range. The background signal was directly subtracted from the specular signal to obtain the corrected intensity. The

(18) Russell, T. P. *Physica B* **1996**, *221*, 267.
(19) Penfold, J. *Curr. Opin. Colloid Interface Sci.* **2002**, *7*, 139−147.
(20) Mezei, F.; Goloub, R.; Klose, F.; Toews, H. *Physica B* **1995**, *213/214*, 898−900.
(21) http://www.hmi.de/bensc/instrumentation/instrumente/v6/v6.html.
(22) Gupta, M.; Gutberlet, T.; Stahn, J.; Keller, P.; Clemens, D. *Pramana-J. Phys.* **2004**, *63*, 57−63.
(23) Clemens, D.; Gross, P.; Keller, P.; Schlumpf, N.; Konnecke, M. *Physica B* **2000**, *276*, 140−141.
(24) http://sinq.web.psi.ch/sinq/instr/amor.html.

reflectivity data were footprint-corrected for the varying flux on the sample as θ increased.

The information that can be extracted in a single NR experiment includes the film thickness, d, the scattering length density profile, $\rho(z)$, across the film, and the surface roughness, σ, between the different layers. The experimentally obtained reflectivity curves were analyzed by applying the standard fitting routine, Parratt 32.[25] It determines the optical reflectivity of neutrons from planar surfaces using a calculation based on Parratt's recursion scheme for stratified media.[26] The film is modeled as consisting of layers of specific thickness, scattering length density, and roughness, which are the fitting parameters. The model reflectivity profile is calculated and compared to the measured one, then the model is adjusted by a change in the fitting parameters to best fit the data. For large enough Q values, the layer thickness, d, can be estimated from the spacing of the minima of two neighboring interference fringes ΔQ, by $d \approx 2\pi/\Delta Q$.

Results and Discussion

We studied the formation of DMPC layers at the interface between PEM and the aqueous phase (D_2O). Two systems were explored to get better insights into the adsorption process: positively charged PAH terminated PEM (sample dP^+) and negatively charged PSS terminated PEM (sample dP^-).

The reflectivity from a semiinfinite substrate decreases monotonically proportional to Q^{-4}. When a layer of a certain material is deposited onto the bare interface, the reflectivity profile $R(Q)$ decreases with oscillations with a period, depending on the thickness of the layer. The amplitude of the oscillations depends on the differences in the SLD of the adjacent phases. The system under consideration in our study consists of a Si block with adsorbed PE layer on top, which is in contact with a reservoir of D_2O. If the SLD of the PEM is close to that of pure D_2O, the SLD profile of an idealized PEM/D_2O interface will exhibit a minor step. Since such an interface is barely visible for neutrons, the reflectivity curve is dominated by the Si/PEM interface and exhibits a Q dependence that follows closely the Q^{-4} dependence characteristic of simple sharp interfaces. The existence of a lipid layer with low SLD at the PEM/D_2O interface will cause a local minimum in the SLD profile, and thus, this interface becomes visible for the neutrons. The interference of neutrons scattered at the Si/PEM and the lipid/D_2O interfaces gives rise to a series of oscillations with pronounced maxima and minima in $R(Q)$ (Kiessig oscillations). In this scattering geometry, the appearance of Kiessig fringes is a sensitive indication of changes at the PEM/D_2O interface. If some of the interfaces in the sample are rough, then the border between the layers smears out, which also results in a decrease in the amplitude of the Kiessig fringes or their disappearance. We used partially deuterated PEM (only the PSS compound was deuterated) that ensures formation of PEM with high SLD, which after swelling in D_2O possesses SLD close to that of the pure D_2O. This way, the reflectivity curves from the bare PEM in D_2O show no Kiessig fringes or only with low amplitude.

Sample dP^+. The reflectivity curves for the positively charged PAH-terminated PE multilayer are shown in Figure 2. Curve 1 was obtained for the bare PEM/D_2O interface. The detailed fit to the data (fitting parameters are summarized in Table 1) shows formation of a PE layer with a thickness of 29.8 nm and SLD 5.51×10^{-6} Å^{-2}. These values are typical for PEM of PAH/d-PSS soaked with D_2O and, for conditions comparable to ours, are very similar to those published in the literature.[27]

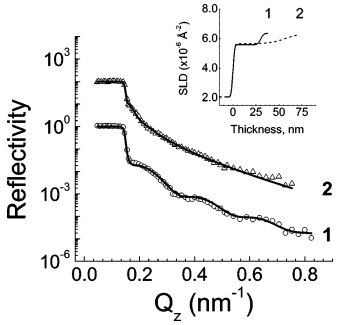

Figure 2. NR curves from the sample dP^+; Si/PEI/(PSS/PAH)$_6$ in D_2O (1, ○) before and (2, △) after DMPC adsorption. The solid curves show the best fits to the experimental data. The curves are shifted for clarity. Inset: the SLD profiles normal to the interface of the film that give the best fits to the data. The numbers have the same meaning as in the main graph.

Table 1. Fitting Parameters Which Give Best Fit to the Experimental Reflectivity Curves for Samples DP^- and DP^+ before and after the Lipid Deposition

	before lipid deposition		after lipid deposition	
layer	thickness d (nm)	SLD ($10^{-6} \times$ Å^{-2})	thickness d (nm)	SLD ($10^{-6} \times$ Å^{-2})
dP^+	29.8 ± 0.7	5.51 ± 0.06	formation of roughlipid layer which does not allow data treatment	
DMPC				
dP^-	31.4 ± 1.2	5.69 ± 0.05	31.4 ± 0.4	4.68 ± 0.23
DMPC			5.0 ± 0.3	0.92 ± 0.14

Curve 2 in Figure 2 was recorded after the deposition of DMPC. Whereas the absorption of a protonated lipid with low SLD[28] should lead to better-pronounced Kiessig fringes in the reflectivity curve, a smearing out of the oscillations is observed. The DMPC interacts with the PE layer, and by arrangement of the lipid molecules in irregular structures, a rough outer lipid layer is most probably created. It smears out the border between the PEM and D_2O, and thus, any oscillations are excluded. The SLD distributions in the sample before and after the lipid deposition are shown as inset in Figure 2. The shape of curve 2 does not allow precise treatment that gives information about the organization of the lipid layer. The SLD profile, which is related to this curve, demonstrates one of the possible estimations. It should be accepted more as a rough approximation than as an exact physical model.

Sample dP^-. Another set of experiments studied the adsorption of DMPC onto a negatively charged d-PSS-terminated PE layer. The reflectivity curves are shown in Figure 3. Curve 1 corresponds to the bare PEM deposited on top of the substrate. The fringes are smeared out similar to those in the case of the dP^+ sample. This is expected according to the lack of contrast (small difference in the SLD) between the deuterated PE layer and the D_2O reservoir. It is nevertheless possible to fit the data using a single box model for the 14-layers-thick d-PSS-

(25) Braun, C. *Parratt 32 Program for Reflectivity Fitting*; Hahn-Meitner Institut: Berlin, 1999.

(26) Parratt, L. G. *Phys Rev* **1954**, *95*, 359−369.

(27) Steitz, R.; Findenegg, G.; Schemmel, S. *Experimental Report*; HMI: Berlin, 2003.

(28) The scattering length in Å^{-2} kg^{-1} m^3 of each compound can be calculated as a sum of the scattering lengths, b_i, of the individual atoms which are tabulated (Sears, V. F. *Neutron News* **1992**, *3*, 26). The determination of the SLD $\rho = [DN_A/M] \sum_i N_i b_i$ (here, D is the bulk density, N_i is the number of certain atoms in the molecule, M is the molar mass, and N_A is Avogadro's number) expressed in Å^{-2} is remarkably sensitive to the value of the density used in its calculation, and a reliable knowledge of the density is a prerequisite for a reliable calculation. Considering the volume of one single DMPC molecule to be around 1050 Å^3, a SLD of 0.93×10^{-6} Å^{-2} was calculated for a layer of DMPC molecules.

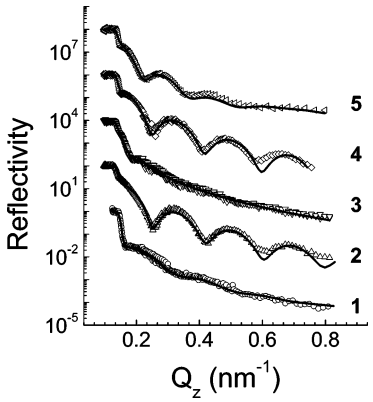

Figure 3. NR curves from the sample dP⁻: Si/PEI/(PSS/PAH)$_6$/d-PSS in D_2O (1, ○) before and (2, △) after DMPC adsorption, (3, ▽) after subsequent d-PSS adsorption, (4, ◇) after subsequent PAH adsorption, and (5, △) after subsequent d-PSS adsorption. The solid curves show the best fit to the experimental data. The numbers of the curves correspond to the numbers of the samples as shown in Table 2. The curves are shifted for clarity.

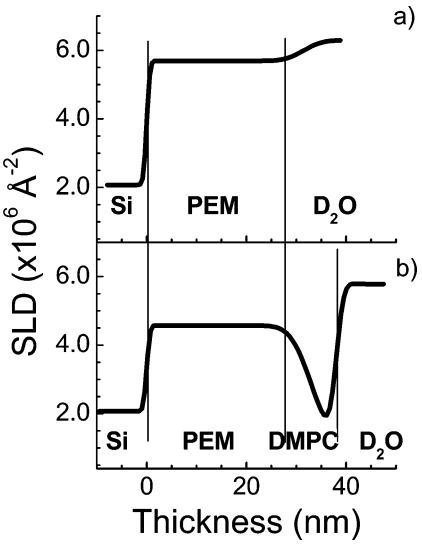

Figure 4. (a) SLD profile normal to the interface of the bare d-PSS terminated sample and (b) SLD profile of the same sample but after the deposition of DMPC.

terminated PE block. Its thickness is 31.4 nm, and the SLD is 5.69×10^{-6} Å^{-2} (see Table 1). The best fit to the data is shown in Figure 3 as a solid line (curve 1). The SLD distribution in the film is shown in Figure 4a. The thickness of the PEM increases in comparison with the PE block of sample dP⁺ with 16 Å, which is a reasonable value for the thickness of a single layer of added PSS.[29] The sample shows high roughness of ~3 nm (see Figure 4a) due to formation of a fuzzy interface with many loops and tails of the polyelectrolytes.

Well-pronounced fringes appear on the reflectivity curve 2 after the deposition of DMPC, which suggests the apparition of a better contrast between the D_2O subphase and the deposited PE film. The best fit to the NR curve is shown as a line in Figure 3 (curve 2), and the corresponding SLD distribution normal to the film interface is presented in Figure 4b. The first part of the profile corresponds to the Si substrate, followed by the PE block. Its thickness is equal to that of the bare PE layer with a thickness of 31.4 nm, but its SLD is decreased to 4.68×10^{-6} Å^{-2}. On top of this first layer, a 5.0-nm-thick layer with a very low SLD of 0.92×10^{-6} Å^{-2} is formed. This value is typical for hydrocarbon compounds, such as DMPC.[8,28] We conclude that this second box corresponds to a DMPC layer adsorbed onto the PE film. Some authors decomposed the fit of NR curves to distinguish the polar headgroup from the lipid tail in the lipid molecules,[11] but this method was not considered in the present paper. The thickness of the DMPC layer corresponds well to the thickness of a single lipid bilayer in the fluid phase at the solid−liquid interface (5.2 nm[30] for a single bilayer, 5.0 nm[31] and 4.7 nm[32] for multibilayer structures).

Some arguments explain the fact that a continuous smooth lipid bilayer could be obtained on top of PSS but not on the top of PAH-terminated PEM. First, the electrostatic argument can be invoked: even if the DMPC is zwitterionic, its headgroup is partially positively charged (see Figure 1) and can be attracted by the negative PSS surface. Moreover, PSS is more hydrophilic than PAH.[33] The polar headgroups of DMPC are known to be surrounded by a hydration layer. This might facilitate the attraction between the DMPC bilayer and the PSS-terminated PEM. Second, the deposition of polycations, such as PAH, leads to formation of a flatter PE layer than in the case of polyanions, such as PSS.[29,34] Consequently, the hydrated loops of PSS may constitute more attractive binding sites than the flat PAH layer.

A strong decrease in the SLD of the PE layer for sample dP⁻ is observed after the deposition of the lipid layer. The measured SLD of the PE layer is the sum of the SLD of the individual components in the film.

$$\rho_{\mathrm{PEM}}^{\mathrm{measured}} = \alpha\rho_{\mathrm{D_2O}} + (1-\alpha)\rho_{\mathrm{PEM}} \qquad (1)$$

Here, α is the volume fraction of D_2O in the film with SLD $\rho_{D_2O} = 6.36 \times 10^{-6}$Å^{-2}. The SLD of the PEM in dry dense state (ρ_{PEM}) was estimated to be 3.35×10^{-6} Å^{-2}.[35] The only variable parameter in eq 1 is the volume fraction α. The decrease in the measured SLD of the PEM may be a result of a decrease in the ratio between the volume fractions of D_2O and polymer in the PEM. The following effects may explain the observed behavior of the PEM.

The NR data for the sample before lipid deposition show high roughness at the dP⁻/D_2O interface (see Figure 4a). This observation correlates with the fact that the PEM in water shows a fuzzy interface with many loops and tails of the polyelectrolytes. When a DMPC bilayer is self-assembled on the PEM, it "compresses" the PE chains into the PEM block, and the interface between the PEM and the lipid layer becomes sharper (see Figure 4b). Thus, the thickness of the PEM film does not change, but the film is more densely packed, which may cause D_2O release.

Another effect may also contribute to the explanation of the observed result. It was recently found[29] that the fraction of D_2O in PEM made by PSS and PAH depends on the charge of the last adsorbed layer. The amount of D_2O in PSS-terminated PEM decreases on adsorption of

(29) Carièrre, D.; Krastev, R.; Schönhoff, M. *Langmuir* **2004**, *20*, 11465−11472.
(30) Salamon, Z.; Tollin, G. *Biophys. J.* **2001**, *80*, 1557−1567.
(31) Mennicke, U.; Salditt, T. *Langmuir* **2002**, *18*, 8172−8177.
(32) Pabst, G.; Katsaras, J.; Raghunathan, V. A.; Rappolt, M. *Langmuir* **2003**, *19*, 1716−1722.
(33) Wong, J. E.; Rehfeldt, F.; Hänni, P.; Tanaka, M.; Klitzing, R. V. *Macromolecules* **2004**, *37*, 7285−7289.
(34) Messina, R.; Holm, C.; Kremer, K. *Langmuir* **2003**, *19*, 4473−4482.
(35) The SLD of the dry film was calculated under the following assumptions: (i) the molecular volumes (V) of the two components are $V_{PSS} \sim 240$ Å^3 and $V_{PAH} \sim 75$ Å^3 (Schmitt, J.; Gruenewald, T.; Decher, G.; Pershan, P. S.; Kjaer, K.; Loesche, M. *Macromolecules* **1993**, *26*, 7058) which corresponds to bulk density $D \sim 1.24$ g × cm^{-3}; (ii) the density of d-PSS is assumed equal to that of h-PSS; (iii) the ratio PAH/d-PSS in the dry interdigitated PEM is 1:1.

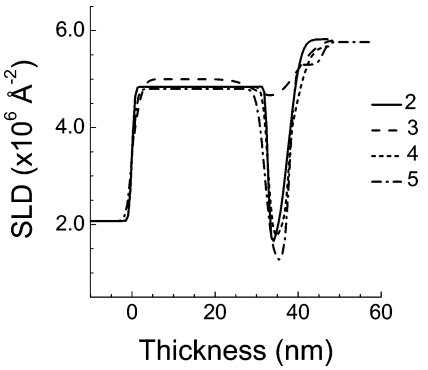

Figure 5. SLD profiles normal to the interface of the sample after the deposition of the PE layers on top of the lipid layer. The numbers of the curves correspond to the numbers of the samples as shown in Table 2. The SLD profile of sample 2 (dP$^-$/DMPC) is given for comparison.

a PAH layer. The water in the hydration shell of the PE, which forms the PEM, is attracted because of mutual electrostatic interaction with the uncompensated polyanion charges. On adsorption of the weaker polycation PAH, part of the negative charges in the PSS are compensated, and thus, the hydration of the PEM decreases. A similar effect may appear in the case of DMPC adsorption. DMPC is a zwiterrionic lipid, but its headgroup is partially positively charged. Its molecules bind electrostatically to the last PSS layer of the PEM, compensating part of the negative charges in the PSS chains. This may generate D_2O release from the PEM block. The PEM consists of a PE matrix with some voids in it. D_2O may be included either in the matrix or in the voids. If D_2O is released only from the voids, the film thickness will stay constant, an effect which we observed.

A third hypothesis may also be considered when one discusses the observed decrease in the SLD of the PEM block after the DMPC deposition. It is possible that the lipid which possesses low SLD penetrates in the PEM block. Thus, it may partially exchange the D_2O. We suppose that this mechanism is less probable. It has to lead to nonhomogeneous distribution of the SLD normal to the PEM surface being lower near to the D_2O/PEM interface and increasing toward the Si/PEM interface. However, the results of the fitting shows existence of PEM block with constant SLD and adsorbed DMPC layer on top of it forming sharp interface.

Formation of PEM/Lipid/PEM Multilayer Structures. Because the in situ deposition of a single lipid bilayer on top of the d-PSS terminated PE block was successful, the deposition of further PE layers on top of the obtained system was investigated. Reflectivity curves 3−5 in Figure 3 correspond to the successive deposition of d-PSS; PAH; and finally, d-PSS again. The full lines represent the best fits to the data, which corresponds to the SLD distribution profiles given in Figure 5.

Adsorption of d-PSS onto the lipid bilayer should not lead to changes in the reflectivity curve because this additional layer possesses a SLD similar to that of the subphase. One has to expect pronounced oscillations in the reflectivity curve because of the deep SLD minimum caused by the lipid layer (Figure 4b). However, curve 3 shows only weak oscillations. Most probably, the PE layer forms a very rough interface or even might disturb the organization of the lipid molecules in the lipid bilayer. Thus, the Kiessig oscillations in the curve are smeared out. It is difficult to extract reliable data about the SLD distribution in the film from the original neutron reflectometry curve. One possible profile is shown in Figure 5 (curve 3), which has to be accepted as only a rough estimate. The buildup process was continued with deposition of a PAH layer. Many well-defined oscillations are observed on curve 4, which proves that the adsorption of a protonated PAH layer onto the d-PSS layer is successful and forms well-ordered and smooth PE (d-PSS/PAH) bilayer. Further deposition of d-PSS layer leads to a change in the reflectivity curve (curve 5 in Figure 3). The positions of the minima of the fringes are shifted toward smaller Q values, which proves the increase in the total film thickness. The decrease in the intensity of the oscillations at moderate Q values is related to an increase in the interfacial roughness.

The last d-PSS layer was prepared under different conditions, as compared to all other layers. The standard procedure comprises deposition of a layer from the solution of the particular PE followed by intensive rinsing with D_2O and NR experiments in the presence of pure D_2O. This procedure was not successful when the last d-PSS layer was adsorbed. The NR experiment did not show formation of any additional layer on top of the last PAH layer. The data shown here were obtained when the solution of d-PSS was kept in the experimental cell during the NR experiment. No adsorption of further layers was possible after that step. This shows that the presence of a DMPC bilayer in the PEM structure disturbs the charge balance in the system. This limits the buildup process to formation of only one PE bilayer. It is also possible that the lipid bilayer increases the hydrophobicity of the whole stack and, thus, disfavors the further growth.

The results of formation of PEM/lipid bilayer/PEM structures are summarized in Table 2. An increase of the overall thickness with every deposition step is noticed. An unexpected high thickness difference between samples 4 and 5 (6.0 nm) can be explained by the formation of a diffuse, last d-PSS layer, probably due to the presence of excess PE in the experimental cell.

Conclusions

In the present study, the formation of model lipid membranes was achieved by absorption of DMPC from extruded vesicular suspensions onto polyelectrolyte multilayer blocks. The PE block was prepared by LbL deposition of the negatively charged PSS and the positively charged PAH. The buildup process was monitored in situ by the use of neutron reflectometry. A 5-nm-thick DMPC layer

Table 2. Overall Thickness of PE/Lipid/PE Multilayer Structures[a]

sample no.	sample structure	overal thickness (nm)
1	Si/PEI/(d-PSS/PAH)$_6$/d-PSS	31.4
2	Si/PEI/(d-PSS/PAH)$_6$/d-PSS**/DMPC**	36.5
3	Si/PEI/(d-PSS/PAH)$_6$/d-PSS**/DMPC/d-PSS**	38.0[b]
4	Si/PEI/(d-PSS/PAH)$_6$/d-PSS**/DMPC/d-PSS/PAH**	40.1
5	Si/PEI/(d-PSS/PAH)$_6$/d-PSS**/DMPC/d-PSS/PAH/d-PSS**	46.1

[a] The overall thickness is a sum of the individual thickness of the PEM block, the lipid layer, and the PE layers adsorbed on top. [b] The value has to be considered as low precise because of the bad quality of the reflectivity curve ($R(Q)$), which is a result of the high roughness of the sample.

was successfully formed after the deposition onto a negatively charged PSS-terminated PE film. Its thickness implies that a lipid bilayer was formed. The positively charged PAH-terminated polymeric block only allows deposition of a rough layer of DMPC. The origin for such behavior might be the electrostatic attraction between the negatively charged d-PSS and the DMPC molecules. Even though DMPC is a zwiterrionic lipid, its headgroup is partially positively charged, and it can be attracted by the negatively charged PSS surface. Another reason might be the nature of the d-PSS, which is more hydrophilic than PAH. This facilitates the attraction between the polar headgroups of the phospholipid, known to be surrounded by a hydration layer, and the PE block. In addition, the deposition of PAH leads to formation of flat layers, whereas those of PSS form hydrated loops, which could constitute attractive binding sites. Deposition of PE layers onto the lipid bilayer was also achieved. This process was successful only for formation of one PSS and one PAH layer after the deposition of the lipid bilayer.

Acknowledgment. C.D. is indebted to the Max-Planck Gesellschaft, the European Doctoral College of the Universities of Strasbourg, and the Région Alsace for financial support. BENSC at HMI, Berlin, Germany is acknowledged for the beam time at the neutron reflectometer V6. Part of this work was performed at SINQ, Paul Scherrer Institute, Villigen, Switzerland, at the neutron reflectometer AMOR. This research project has been supported by the European Commission under the 6th Framework Program through the Key Action: Strengthening the European Research Area, Research Infrastructures, Contract n*o*. RII3-CT-2003-505925 (NMI3). Nadejda Krasteva is acknowledged for the critical reading of the manuscript.

Supporting Information Available: Scheme of the solid/liquid experimental cell used in the neutron reflectometry experiments. This material is available free of charge via the Internet at http://pubs.acs.org.

LA050407N